Surface Science 606 (2012) 1948–1953

Contents lists available at SciVerse ScienceDirect

Surface Science

journal homepage: www.elsevier.com/locate/susc

Formation of nitric oxide dimers on MgO-supported gold particles

Silvia A. Fuente [a], Leandro F. Fortunato [b], Nicolás Domancich [a], Norberto J. Castellani [a], Ricardo M. Ferullo [b,*]

[a] Grupo de Materiales y Sistemas Catalíticos, IFISUR, Departamento de Física, Universidad Nacional del Sur, Av. Alem 1253, 8000 Bahía Blanca, Argentina
[b] INQUISUR, Departamento de Química, Universidad Nacional del Sur, Av. Alem 1253, 8000 Bahía Blanca, Argentina

ARTICLE INFO

Article history:
Received 30 May 2012
Accepted 8 August 2012
Available online 17 August 2012

Keywords:
Au/MgO
Gold clusters
N_2O_2
Nitric oxide
DFT
Cluster model

ABSTRACT

We present density functional theory (DFT) calculations on the formation of nitric oxide dimers (N_2O_2) on Au atoms, dimers and trimers adsorbed on regular O^{2-} sites and neutral oxygen vacancies (F_s sites) of the MgO(100) surface. The study of the N_2O_2 species is of great interest since it has been detected in the NO reduction reaction as an intermediate towards the formation of N_2O. We found that the coupling of a NO molecule with a previously adsorbed one on Au/MgO is energetically favorable on Au_1 and Au_3, but unfavorable on Au_2. The stability of N_2O_2 is in direct relation with the amount of charge taken from the support. Furthermore, one of the N—O bonds can be activated as a result of the attraction between the negatively charged NO dimer and the ionic oxide surface. In fact, for Au_1 anchored on the F_s site a barrierless reaction occurs between N_2O_2 and a third NO molecule, forming adsorbed N_2O and NO_2.

1. Introduction

Gold, a noble metal as bulk material, becomes very active at nano or subnano scale. Used as catalysts, small gold particles supported on oxide surfaces catalyze a wide range of important reactions [1]. In general, in these complex systems the support is not a mere material where the gold particles are dispersed but it can strongly modify their chemical activity due to changes in morphology, size distribution and charge polarization. From a theoretical viewpoint the role of the support in activating gold particles has been studied in oxides like MgO, TiO_2, Al_2O_3 and Fe_2O_3 [2–5].

In theoretical simulations, MgO is commonly used as a model oxide support because it presents different types of crystallographic defects which are relatively easy to represent. The deposition of gold particles on regular and defective MgO(100) surface has been extensively studied in the past by using density functional theory [6–16]. Among the possible defect sites, the most studied has been the F_s one. It is generated by the removal of a neutral O atom from the MgO surface, and consequently, two electrons are trapped inside the cavity. Interestingly, a correlation between these sites and the activity of Au supported catalysts has been found [17]. When Au particles are anchored on F_s sites, a charge transfer occurs from the vacancy to the metal catalyst enhancing the metal–oxide interaction [6,18]. This behavior is particularly relevant in the case of Au because of its high electron affinity.

Nitric oxides (NO_x) are important air pollutants which are formed in automotive engines by thermal oxidation of the nitrogen present in air. The catalytic reduction of NO_x has been a scientific challenge for catalytic research during the last decades. A highly practical and suitable method to remove nitrogen oxides is the catalytic reduction making use of compounds contained in exhaust gases such as carbon monoxide, hydrogen and hydrocarbons. Ueda and Haruta [19] found that Au catalysts supported in a variety of metallic oxides show a high catalytic activity in the reduction of NO with hydrocarbons such as propene, propane, ethene and ethane.

During the reduction of NO to N_2, N_2O was observed as an intermediate product [20,21]. For the formation of N_2O two different mechanisms have been proposed: through the dissociative adsorption of NO [22–24], or via the formation of N_2O_2 [25–28]. In the first case a NO molecule dissociates directly onto the surface to give adsorbed N and O atoms, and then, the N atom reacts with another NO molecule to yield N_2O. In the dimer mechanism, two NO molecules interact to form N_2O_2 through the formation of a N—N bond. In the next step, the dimer dissociates to N_2O and N. Concerning particularly on Au based systems, N_2O_2 has been detected upon NO adsorption on Au supported on TiO_2 [29], zeolites [30], and on Au hemispherical crystals [31]. Recently, Wang et al. performed DFT calculations to study the formation of N_2O on Au(111) according to these mechanisms [28]. They found that while the direct NO dissociation involves a significant activation barrier (about 4 eV), the dissociation mechanism via the dimer is energetically more favorable. On the other hand, the adsorption of NO dimers on MgO(100) was studied using the embedded cluster approach [32]. These calculations showed that the NO molecules and N_2O_2 species adsorb very weakly over this surface. The geometrical structure of N_2O_2 is characterized by a relatively long N—N distance of about 1.8 Å. Moreover the interaction of NO molecules with the surface is strong only at F_s sites. The formation of N_2O_2 is also favored on the vacancies, yielding N_2O with a very low activation barrier.

* Corresponding author. Tel.: +54 291 4595159; fax: +54 291 4595160.
E-mail address: caferull@criba.edu.ar (R.M. Ferullo).

0039-6028/$ – see front matter © 2012 Elsevier B.V. All rights reserved.
http://dx.doi.org/10.1016/j.susc.2012.08.003

On free gold particles having up to 13 atoms NO exhibits the highest adsorption energies for Au_1 and Au_3 [33]. Previously, we have reported a molecular orbital study about the NO interaction with Au atoms, dimers and trimers anchored on the regular MgO(100) surface [18,34]. The results indicate that while the NO interaction with Au_1 and Au_3 is strong, that with Au_2 is energetically unfavorable. We have also studied the NO adsorption on Au_1, the last interacting with a F_s site. It was found that the Au atom adsorbed on anionic sites essentially preserves its spin and for this reason the interaction with the radical NO is relatively strong. Conversely, when the Au atom is adsorbed on a F_s site, the Au—NO bond is weaker due to the spin delocalization into the cavity. In the present theoretical work we continue the study of NO adsorption on Au/MgO model catalysts by analyzing the formation of N_2O_2 as a possible intermediate for the production of N_2O. For that purpose, we have focused our interest to the case of the coupling of a NO molecule with a previously adsorbed one on supported Au, this last molecule maintaining the N—Au link. However, other competitive possibilities cannot be discarded, such as the structure in which the two oxygen atoms are bonded with Au, or the simultaneous adsorption of two NO molecules on a Au atom. As a first approach to this problem, O^{2-} and F_s adsorption sites of MgO were modeled considering the (100) terraces of this oxide.

2. Computational details

Density functional theory (DFT) calculations were performed using the gradient corrected Becke's three parameters hybrid exchange functional in combination with the correlation functional of Lee, Yang and Parr (B3LYP) [35]. All the calculations were carried out using the Gaussian-03 program package [36]. As in previous works [18,34,37] the MgO(100) surface was represented using the embedding technique, widely used for ionic solids, in which a cluster is embedded by an array of ± 2 point charges. Furthermore, the positive point charges at the interface between the cluster region and the point charge region were replaced by effective core potentials (ECP), corresponding to the Mg^{2+} cation, in order to account for its finite size and to avoid spurious charge polarization. The cluster used in this study can be expressed more specifically through the formula $Mg_{13}O_{13}$(Mg-ECP)$_{16}$.

The 6-31 + G(d) basis set was employed for the atoms of NO molecules and the O atoms in the first layer of the $Mg_{13}O_{13}$ cluster, except for the terminal ones. The atomic orbitals of the four Mg atoms in the first layer were described by the 6-31G(d) basis set, while those of terminal O atoms and those of Mg and O atoms at the second layer, by the 6-31G basis set. For Au, the LANL2DZ basis set was used. During the geometrical optimization procedure, the coordinates of atoms belonging to the adsorbates (both NO and Au), and those of the five central atoms in the first layer of the $Mg_{13}O_{13}$ cluster (the central O and the four Mg atoms directly bonded to it) were fully optimized. The neutral O vacancy was represented by the $Mg_{13}O_{12}$(Mg-ECP)$_{16}$ cluster, with the vacancy localized in the center of the first layer. In this case, the geometrical optimization included only the four central Mg atoms of first layer. Previous studies have demonstrated that the reconstruction of the lattice around the F_s site is negligible [15,38] so that this geometric constraint can be considered as a good approximation. It is well established that on surfaces the oxygen vacancies are mainly located on low-coordinated sites [39]; nevertheless, extended surfaces representing terraces are usually used as idealized systems in order to make qualitative comparative studies of the different behavior between F_s and O^{2-} sites as adsorption centers [8,9,12–15,40–43]. The notations "Au_n/O^{2-}" and "Au_n/F_s" for gold supported on an anionic site and on a vacancy, respectively, will be used.

The NO dimer formation energy was defined as $E_{dim} = -[E(N_2O_2/Au_n/MgO, site) - E(NO/Au_n/MgO, site) - E(NO)]$, with $n = 1$, 2 or 3, and site = O^{2-} or F_s. Thus, this energy is associated to the coupling of an incoming NO molecule with a preadsorbed one on Au_n/MgO. Defined in this way, positive values correspond to exothermic processes. These energies were corrected by considering the basis set superposition error (BSSE), calculated according to the counter-poise (CP) correction [44]. All the other calculated adsorption energies presented throughout the text were also CP-corrected.

N—O vibrational frequencies were computed by determining the second derivatives of the energy with respect to the Cartesian nuclear coordinates and then transforming to mass-weighted coordinates. The frequency values were scaled according to the factor of 0.9465, calculated as the ratio between the empirical and the calculated frequency values for the isolated NO molecule (1876/1982). The net atomic charges and spin populations were calculated following the natural bond orbital (NBO) scheme [45].

3. Results and discussion

We begin our study with the formation of NO dimer on supported Au atoms attached to regular anionic and oxygen vacancy sites. The first step for this reaction is obviously the interaction of NO with supported gold, already treated in previous investigations [18]. As explained in Introduction, this interaction is stronger when the adsorption takes place on a Au atom anchored on the O^{2-} site than on the F_s site, with adsorption energies of 1.08 and 0.49 eV, respectively.

From a geometrical point of view, the incoming NO can interact with the previously absorbed one in two different ways giving either *cis* or *trans* configurations. Some selected numerical results are presented in Table 1 and the corresponding geometrical configurations are schematized in Fig. 1. For both sites the *trans* configuration is more stable by about 0.1 eV. On the other hand, the dimer formation energy is considerably higher on Au_1/F_s than on Au_1/O^{2-} (about 0.9 eV). Moreover, in both cases, the adsorbed N_2O_2 molecule acquires electronic charge from the substrate (in the range of −0.6 to −0.9|*e*|), the effect being more significant for Au_1/F_s. This relationship between the dimer stability and its charge was already observed for the free species. Indeed, the isolated N_2O_2 molecule exhibits a very small formation energy at neutral state. However, the dimer has a high electron affinity and becomes considerably stabilized when it takes an electron, giving the $N_2O_2^-$ anion [46]. This stabilization is accompanied with a noticeable shortening of the N—N distance owing to the occupation of the $2b_1$ orbital of N_2O_2, which presents a very strong N—N bonding character [47]. The shorter N—N distance obtained in Au_1/F_s (Fig. 1) can be related with the larger amount of negative charge taken by the dimer. We

Table 1
Dimer formation energies (E_{dim}), electronic charges (q), spin populations and stretching frequencies (ν) for N_2O_2 adsorbed on Au atoms attached to surface O^{2-} sites and to F_s sites.

	O^{2-}		F_s	
	cis	*trans*	*cis*	*trans*
E_{dim} (eV)	0.83	0.96	1.71	1.86
q[Au] (|*e*|)	0.44	0.42	−0.54	−0.54
q[N(1)]	0.00	0.00	−0.09	−0.07
q[O(1)]	−0.34	−0.34	−0.52	−0.63
q[N(2)]	0.11	0.13	0.08	0.11
q[O(2)]	−0.33	−0.37	−0.36	−0.31
$q(N_2O_2)$	−0.56	−0.58	−0.89	−0.90
Spin pop. [Au_n]	0.00	0.00	0.00	0.00
Spin pop. [N(1)]	0.24	0.19	0.27	0.23
Spin pop. [O(1)]	0.41	0.45	0.36	0.38
Spin pop. [N(2)]	0.06	0.04	0.04	0.02
Spin pop. [O(2)]	0.29	0.33	0.34	0.37
Spin pop. [N_2O_2]	1.00	1.00	1.00	1.00
ν_{NOsym}[a] (cm^{-1})	1416	1391	1328	1337
ν_{NOasym}[b]	1328	1309	1234	1246
ν_{NN}	675	924	735	960

[a] N—O symmetric stretching mode.
[b] N—O asymmetric stretching mode.

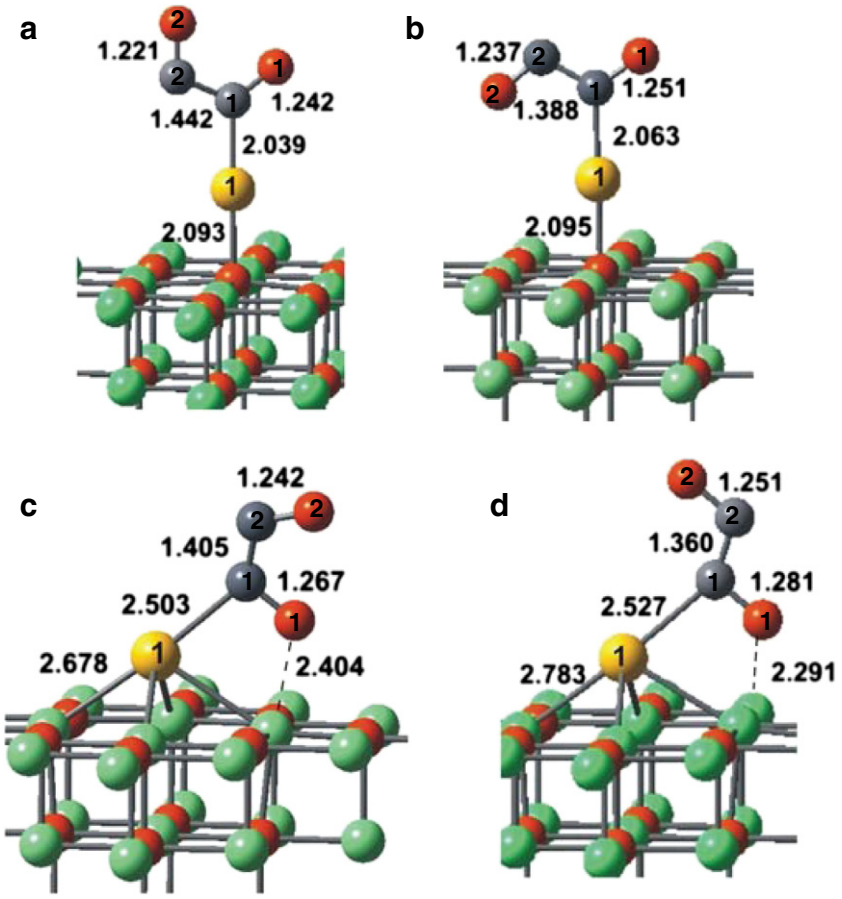

Fig. 1. Schematic representations of N_2O_2 adsorbed on a gold atom attached to a surface O^{2-} site (a and b), and to a F_s site (c and d). Red spheres: O. Green spheres: Mg. Yellow spheres: Au.

note that the formation of stable anionic NO dimers was also predicted on BaO and CaO surfaces [47,48].

The capability to transfer electronic charge to N_2O_2 from the support is in direct relation with the energetic position of the high singly occupied molecular orbital, commonly referred as SOMO, of the Au_1/MgO systems. Indeed, while in Au_1/F_s the SOMO is at −1.2 eV (the MOs immediately below it lie at about −4.5 eV), in the Au_1/O^{2-} system the SOMO is considerably more stable, located at about −3.8 eV (with the MOs immediately below at about −5.3 eV). According to these electronic configurations it is clear that the charge transfer should be more facilitated in the presence of vacancies.

Another interesting observation is the different orientation adopted by adsorbed N_2O_2. On Au_1/F_s the dimer is tilted towards the surface due to the bonding established between an O of the dimer (labeled as O(1) in Fig. 1) and an Mg cation. This interaction of ionic nature is present only at Au_1/F_s because of the larger amount of negative charge present in this O atom (reaching to −0.63|*e*| in *trans* configuration, Table 1). As a consequence, the corresponding N—O bond (labeled as N(1)—O(1) in Fig. 1) is longer in comparison with the adsorption on Au_1/O^{2-}. This implies a likely activation of this N—O bond, either to dissociate directly onto the surface or to react with other species such as another NO molecule. Inspection of Table 1 shows that the spin is entirely localized on the dimer, and particularly concentrated on the O atoms (about 70% of spin), a fact that favors the interaction with a radical such as NO.

Looking at the vibrational frequency values summarized in Table 1, the N—O stretching modes for the adsorption on Au_1/F_s lie in the range of 1230–1340 cm^{-1}, while on Au_1/O^{2-} they are comprised in the interval of 1310–1420 cm^{-1}. This implies a significant shift with respect to the frequency calculated for the isolated NO molecule (1876 cm^{-1}). Concerning the N—N stretching mode, we notice that the values on Au_1/F_s are higher (by around 40 to 60 cm^{-1}) in line with the above commented shorter N—N distances.

Table 2
Dimer formation energies (E_{dim}), electronic charges (q), spin populations and stretching frequencies (ν) for N_2O_2 adsorbed on Au_2 and Au_3 attached to surface O^{2-} sites and to F_s sites.

	N_2O_2/Au_2/MgO		N_2O_2/Au_3/MgO	
	O^{2-}	F_s	O^{2-}	F_s
E_{dim} (eV)	−0.12	0.05	0.91	0.93
q[Au(1)] (|e|)	0.00	−0.29	0.24	−0.64
q[Au(2)]	0.02	−0.17	−0.08	−0.35
q[Au(3)]	–	–	0.26	0.21
q[Au_n]	0.02	−0.46	0.42	−0.78
q[N(1)]	0.04	0.08	−0.03	−0.03
q[O(1)]	−0.24	−0.40	−0.37	−0.41
q[N(2)]	0.23	0.21	0.14	0.13
q[O(2)]	−0.19	−0.27	−0.34	−0.34
q(N_2O_2)	−0.16	−0.38	−0.60	−0.65
Spin pop. [Au_n]	0.00	0.00	0.00	0.01
Spin pop. [N(1)]	0.00	0.00	0.19	0.21
Spin pop. [O(1)]	0.00	0.00	0.45	0.44
Spin pop. [N(2)]	0.00	0.00	0.00	0.00
Spin pop. [O(2)]	0.00	0.00	0.33	0.33
Spin pop. [N_2O_2]	0.00	0.00	0.97	0.98
ν_{NOsym}[a] (cm^{-1})	1724	1586	1390	1393
ν_{NOasym}[b]	1586	1402	1331	1325
ν_{NN}	741	766	905	906

[a] N—O symmetric stretching mode.
[b] N—O asymmetric stretching mode.

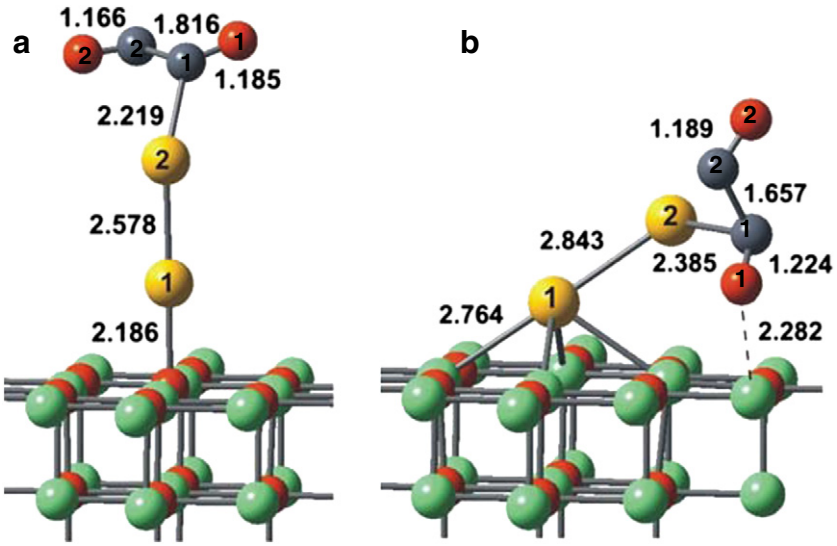

Fig. 2. Schematic representations of N_2O_2 adsorbed on Au_2 attached to a surface O^{2-} site (a), and to a F_s site (b). Red spheres: O. Green spheres: Mg. Yellow spheres: Au.

Regarding the adsorption of N_2O_2 on Au_2/MgO and Au_3/MgO some selected numerical results are presented in Table 2 and the corresponding geometrical configurations are schematized in Figs. 2 and 3, respectively. Particularly, taking into account the more stable structure attained on supported gold atoms, in the following only the *trans* configuration will be considered.

NO adsorbs on Au_2 supported on both regular and defective MgO(100) with adsorption energies of about 0.2 eV [18]. The coupling with another NO molecule to form the dimer is thermodynamically unfavorable (Table 2). The HOMOs in the Au_2/O^{2-} and Au_2/F_s systems are located at about −5 and −4 eV, respectively; hence, the charge transfer to adsorbed molecules is energetically a rather difficult process. Consequently, as it can be observed from Table 2, the dimer acquires less negative charge (in the range of −0.2 to −0.4|*e*|) in comparison with supported Au atoms. The significantly longer N—N distances and smaller N—N stretching frequencies reported in Fig. 2 and Table 2, respectively, are in agreement with the low stability of adsorbed N_2O_2.

We now turn to consider the adsorption of one NO molecule on supported Au_3. Previous calculations performed on NO adsorption over Au_3/O^{2-} showed an adsorption energy value of 0.87 eV [34]. To complete this scheme, the corresponding value for Au_3/F_s was computed obtaining a very similar result of 0.84 eV. The optimized geometry and some selected results for the formation of N_2O_2 on supported Au_3 are presented in Fig. 3 and Table 2. It is interesting to note that the dimerization energies (about 0.9 eV) as well as the orientation and distances of optimized geometries are very similar on both Au_3/O^{2-} and Au_3/F_s.

Conversely to the case of supported Au_1, the charge of N_2O_2 is very similar if we compare Au_3/O^{2-} with Au_3/F_s (−0.60 and −0.65|*e*|, respectively; Table 2). In these systems the energetic positions of the SOMOs are quite similar; it is at −3.8 eV in Au_3/O^{2-} and at −3.1 eV in Au_3/F_s (the levels immediately below lie at about −5.4 and −4.1 eV, respectively). From Table 2 we notice also that, analogously to the N_2O_2/Au_1/MgO systems, for N_2O_2/Au_3/MgO the spin is mainly concentrated on the O atoms.

For the sake of comparison, we carried out complementary calculations concerning the formation of N_2O_2 on non-supported neutral gold particles (*trans* configuration). The E_{dim} values resulted to be 0.08, −0.06 and 0.41 eV for Au_1, Au_2 and Au_3, respectively. Thus, while the formation is also unfavorable on Au_2, the results on Au_1 and Au_3 show an enhancement due to the support, this effect being very remarkable on Au_1/F_s. The corresponding N_2O_2 charges were −0.31, +0.03 and −0.51 eV, respectively, revealing a less noticeable

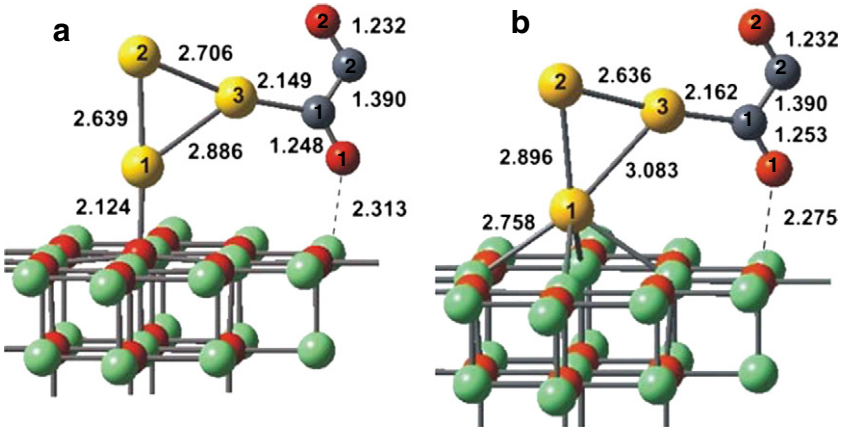

Fig. 3. Schematic representations of N_2O_2 adsorbed on Au_3 attached to a surface O^{2-} site (a), and to a F_s site (b). Red spheres: O. Green spheres: Mg. Yellow spheres: Au.

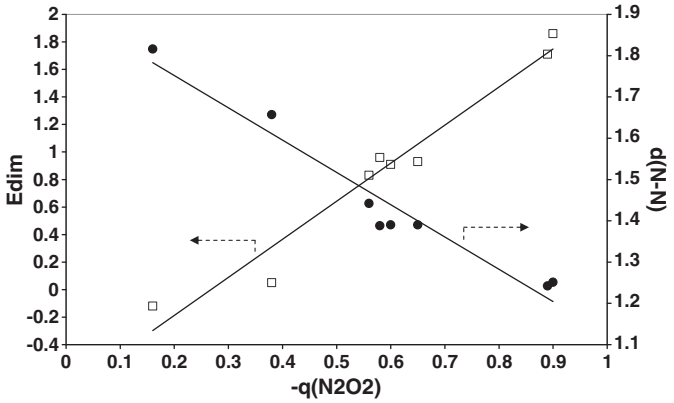

Fig. 4. Negative charge of N_2O_2 as a function of the dimer formation energy (E_{dim}, in eV), and of the N—N distance (in Å). Trend lines are obtained by linear regression.

negative polarization of N_2O_2 molecule than that of the supported Au systems.

In Fig. 4 the E_{dim} energies and N—N distances taken from Tables 1 and 2 and Figs. 1–3, respectively, are plotted as a function of the net (negative) charge of N_2O_2 molecule. It is outstanding the good correlation attained between these molecular parameters, following the ideas commented in previous paragraphs, and suggesting the important role that could be played by the electronic charge transfer to an adsorbed molecule in other supported Au systems. Notice that low dimerization energies correlate with long N—N distances and poor electronic charge transfers to N_2O_2, while high dimerization energies with short N—N distances and large charge transfers.

When monomeric NO is adsorbed, the spin is mainly located on N, as it was observed upon NO adsorption on supported gold particles [18,34]. However, in $N_2O_2/Au_1/MgO$ and $N_2O_2/Au_3/MgO$ systems, spin populations present larger values on the O atoms (Tables 1 and 2). This spin distribution should make the dimer very reactive against a third NO molecule (a radical). For example, the dimer could react with another NO molecule, either from gas phase or as an adsorbed species, according to:

$$ONNO + NO \rightarrow N_2O + NO_2.$$

In relation with this peculiar spin distribution, the effect of the support for the activation of the N—O bond is likely to be significant because in some cases considered here, particularly Au_1/F_s, Au_3/O^{2-} and Au_3/F_s, the adsorbed N_2O_2 molecule presents a large negative charge. In these situations, the dimer interacts with the ionic oxide surface through the bond established between an O atom of N_2O_2 and an Mg^{2+} ion, resulting in an activated N—O bond. To explore this situation we modeled the coadsorption of the dimer with a third NO molecule, only for adsorbed Au atoms on O^{2-} and F_s sites. These systems were chosen because they present quite different dimer formation energies and geometric structures. We start, for both cases, with the N_2O_2 molecule oriented similarly than that presented in Fig. 1b, and with another NO molecule adsorbed on the surface. The initial distance between the last NO molecule and the nearest O of the dimer is about 2.8 Å. The optimized final structures are shown in Fig. 5. While on Au_1/O^{2-} the dimer carries the NO away from the surface, on Au_1/F_s one of the N—O bonds of N_2O_2 is broken to form N_2O. Actually, the $N_2O\cdots NO_2$ adsorbed complex is formed previously to the complete releasing of these molecules. Notice that the geometrical structure of N_2O is not lineal as in gas phase due to the attraction exerted by the support (Fig. 5).

4. Conclusions

DFT calculations on the formation of NO dimers on Au_1, Au_2 and Au_3 adsorbed on regular O^{2-} sites and neutral oxygen vacancies (F_s sites) of the MgO(100) surface were carried out. The coupling of two NO molecules interacting with Au via Au—N bonds was only explored, not excluding the existence of other minima on the potential energy surface.

i) NO couples very strongly with another previously adsorbed NO molecule on Au_1/F_s with an adsorption energy of about 1.9 eV. On Au_1/O^{2-}, Au_3/O^{2-} and Au_3/F_s the interaction is less favorable but still strong, with values of about 0.9–1.0 eV. On Au_2 the interaction is very weak.

ii) The NO dimer stability presents a direct correlation with the amount of negative charge of N_2O_2. As this charge increases, the stability increases and the N—N distance decreases. At the same time, the charge transfer from the support to the dimer is related to the energetic position of the highest singly occupied molecular orbital of the Au_n/MgO system ($n = 1$–3).

iii) The support can play an important role in activating one of the N—O bonds of the dimer. In particular, in Au_1/F_s, a strong bond of ionic character is established between one of the O terminal atoms of the dimer and the Mg^{2+} ion, producing a weakening of this N—O bond. Besides, the spin is mainly concentrated on the terminal O atoms of N_2O_2. For this reason the dimer, apart from its possibility to dissociate over the surface, can react with another preadsorbed NO molecule to form N_2O and NO_2. Interestingly, this process is observed to be barrierless on Au_1/F_s.

Acknowledgments

The authors acknowledge the financial support of CONICET, ANPCYT and Universidad Nacional del Sur (UNS).

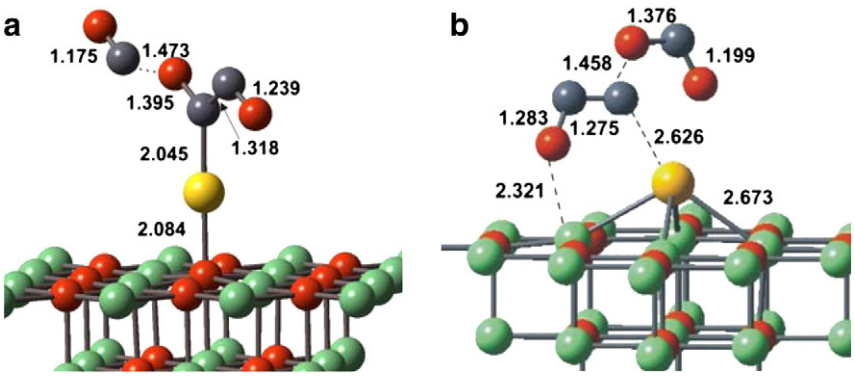

Fig. 5. Optimized structures obtained when a third NO molecule is placed near the NO dimer adsorbed on a gold atom attached to a surface O^{2-} site (a), and to a F_s site (b).

References

[1] G.C. Bond, C. Louis, D.T. Thompson, Catalysis by Gold, Imperial College Press, London, 2006.
[2] A. Roldán, J.M. Ricart, F. Illas, G. Pacchioni, J. Phys. Chem. C 114 (2010) 16973.
[3] P. Ganesh, P.R.C. Kent, G.M. Veith, J. Phys. Chem. Lett. 2 (2011) 2918.
[4] C. Shang, Z.-P. Liu, J. Phys. Chem. C 114 (2010) 16989.
[5] K.L. Howard, D.J. Willock, Faraday Discuss. 152 (2011) 135.
[6] A. Del Vitto, G. Pacchioni, F. Delbecq, P. Sautet, J. Phys. Chem. B 109 (2005) 8040.
[7] M. Sterrer, M. Yulikov, E. Fischbach, M. Heyde, H.P. Rust, G. Pacchioni, T. Risse, H.J. Freund, Angew. Chem. Int. Ed. 45 (2006) 2630.
[8] L.M. Molina, J.A. Alonso, J. Phys. Chem. C 111 (2007) 6668.
[9] P. Frondelius, H. Häkkinen, K. Honkala, New J. Phys. 9 (2007) 339.
[10] P. Frondelius, H. Häkkinen, K. Honkala, Phys. Rev. B: Condens. Matter 76 (2007) 073406.
[11] L.M. Molina, B. Hammer, Phys. Rev. B: Condens. Matter 69 (2004) 155424.
[12] R. Caballero, C. Quintanar, A.M. Köster, S.N. Khanna, J.U. Reveles, J. Phys. Chem. C 112 (2008) 14919.
[13] A. Bogicevic, D.R. Jennison, Surf. Sci. Lett. 515 (2002) L481.
[14] C. Inntam, L.V. Moskaleva, K.M. Neyman, V.A. Nasluzov, N. Rösch, Appl. Phys. A 82 (2006) 181.
[15] G. Barcaro, A. Fortunelli, J. Chem. Theory Comput. 1 (2005) 972.
[16] K.M. Neyman, C. Inntam, A.V. Matveev, V.A. Nasluzov, N. Rösch, J. Am. Chem. Soc. 127 (2005) 11652.
[17] Z. Yang, S. Chinta, A.A. Mohamed, J.P. Fackler, D.W. Goodman, J. Am. Chem. Soc. 127 (2005) 1604.
[18] S.A. Fuente, P.G. Belelli, R.M. Ferullo, N.J. Castellani, Surf. Sci. 602 (2008) 1669.
[19] A. Ueda, M. Haruta, Gold Bull. 32 (1999) 3.
[20] R. Burch, J.P. Breen, F.C. Meunier, Appl. Catal., B 39 (2002) 283.
[21] A.C. Gluhoi, S.D. Lin, B.E. Nieuwenhuys, Catal. Today 90 (2004) 175.
[22] J.F. Wendelken, Appl. Surf. Sci. 11 (12) (1982) 172.
[23] S.K. So, R. Franchy, W. Ho, J. Chem. Phys. 91 (1989) 5701.
[24] H.J. Borg, J.F.C.-J.M. Reijerse, R.A. van Santen, J.W. Niemantsverdriet, J. Chem. Phys. 101 (1994) 10052.
[25] W.A. Brown, P. Gardner, D.A. King, J. Phys. Chem. 99 (1995) 7065.
[26] A. Ludviksson, C. Huang, H.J. Jansch, R.M. Martin, Surf. Sci. 284 (1993) 328.
[27] A. Bogicevic, K.C. Hass, Surf. Sci. Lett. 506 (2002) L237.
[28] Y. Wang, D. Zhang, Z. Yu, C. Liu, J. Phys. Chem. C 114 (2010) 2711.
[29] M.A. Debeila, N.J. Coville, M.S. Scurrell, G.R. Hearne, Catal. Today 72 (2002) 79.
[30] S. Qiu, R. Ohnishi, M. Ichikawa, J. Phys. Chem. 98 (1994) 2719.
[31] T.-D. Chau, T. Visart de Bocarmé, N. Kruse, Catal. Lett. 98 (2004) 85.
[32] C. Di Valentin, G. Pacchioni, S. Abbet, U. Heiz, J. Phys. Chem. B 106 (2002) 7666.
[33] X. Ding, Z. Li, J. Yang, J.G. Hou, Q. Zhu, J. Chem. Phys. 121 (2004) 2558.
[34] S.A. Fuente, R.M. Ferullo, N.F. Domancich, N.J. Castellani, Surf. Sci. 605 (2011) 81.
[35] A.D. Becke, J. Chem. Phys. 98 (1993) 5648.
[36] M.J. Frisch, et al., Gaussian 03, Revision C.02, Gaussian, Inc., Wallingford, CT, 2004.
[37] R.M. Ferullo, S.A. Fuente, P.G. Belelli, N.J. Castellani, Surf. Sci. 603 (2009) 1262.
[38] M. Ménétrey, A. Markovits, C. Minot, A. Del Vitto, G. Pacchioni, Surf. Sci. 549 (2004) 294.
[39] M. Sterrer, E. Fischbach, T. Risse, H.-J. Freund, Phys. Rev. Lett. 94 (2005) 186101.
[40] E. Florez, P. Fuentealba, F. Mondragón, Catal. Today 133–135 (2008) 216.
[41] Y. Wang, E. Florez, F. Mondragón, T.N. Truong, Surf. Sci. 600 (2006) 1703.
[42] Y.F. Zhukovskii, E.A. Kotomin, R.A. Evarestov, D.E. Ellis, Int. J. Quantum Chem. 107 (2007) 2956.
[43] Y. Wang, T.N. Truong, J. Phys. Chem. C 112 (2008) 13674.
[44] S.F. Boys, F. Bernardi, Mol. Phys. 19 (1970) 553.
[45] A.E. Reed, L.A. Curtiss, F. Weinhold, Chem. Rev. 88 (1988) 899.
[46] A. Snis, I. Panas, Chem. Phys. 221 (1997) 1.
[47] R.M. Ferullo, S.A. Fuente, M.M. Branda, N.J. Castellani, J. Mol. Struct. (THEOCHEM) 818 (2007) 57.
[48] C. Di Valentin, G. Pacchioni, M. Bernasconi, J. Phys. Chem. B 110 (2006) 8357.